J. Min. Metall. Sect. B-Metall. 57 (3) (2021) 421 - 430

Journal of Mining and Metallurgy, Section B: Metallurgy

THERMAL PROCESS FOR MAGNESIUM PRODUCTION WITH Al-Si-Fe FROM COAL FLY ASH: THERMODYNAMICS AND EXPERIMENTAL INVESTIGATION

Q.-C. Yu*, Y. Deng, S.-B. Yin, Z.-Y. Li

State Key Laboratory of Complex Nonferrous Metal Resources Clear Utilization, Faculty of Metallurgical and Energy Engineering, Kunming University of Science and Technology, Kunming, P.R. China

(Received 18 January 2021; Accepted 10 July 2021)

Abstract

Dumping or disposal of fly ash causes environmental pollution and huge waste of valuable metals. In this work, carbothermic reduction of fly ash under normal pressure to produce Al-Si-Fe alloy, and thermal reduction of magnesia to produce magnesium in vacuum with Al-Si-Fe alloy were investigated. In addition, the surface morphology and composition of Al-Si-Fe alloy and magnesium were studied by means of SEM-EDS and XRD. Based on the thermodynamic analysis, it was found that AlN and SiO_2 lowered down the reduction temperature of SiC and Al_4C_3, respectively. Increase of temperature and decrease of vacuum degree promotes the thermal reduction of magnesia. Results showed that the recovery rate ranked Fe, Si, and Al in a descending order. The evaporation loss of gaseous SiO and Al_2O reduced the recovery of Si and Al. Al-Si-Fe alloy containing 33.12% Al, 48.73% Si, and 6.41% Fe is obtained under the optimal conditions. Magnesium with the content of 94.87% is prepared using the obtained Al-Si-Fe alloy as a reductant. The nucleation rate is less than the growth rate during the condensation of magnesium vapor.

Keywords: *Coal fly ash; Carbothermic reduction; Aluminothermic reduction; Al-Si-Fe alloy; Magnesium*

1. Introduction

Magnesium is produced by two principal processes: electrolysis of magnesium chloride and thermal reduction of magnesia. Carbothermic reduction of magnesia to produce magnesium is reported experimentally [1]. Among thermal reduction processes, Pidgeon process has made a strong revival, particularly in China during the past few decades [2]. The advantage of Pidgeon process over electrolytic process is that the main source of magnesium is dolomite, which merely requires calcining, unlike the complex purification that the electrolytic route requires to produce anhydrous magnesium chloride feed [3, 4]. Industrially the Pidgeon process for magnesium production is based on the reduction of magnesia with ferrosilicon (Fe-Si). However, in Pidgeon process the reduction pot has a short service life (3–5 months). Additionally, the Pidgeon process consumes significant amount of energy to achieve high temperatures and is highly polluting when it uses fossil fuels [5]. When aluminum is added in the reductant of ferrosilicon, the reduction temperature of magnesia decreases [6]. Coal fly ash is a kind of industrial waste containing lots of Al_2O_3, SiO_2, and small amount of Fe_2O_3 [7], which makes it possible to be used as raw material to produce Al-Si-Fe alloy.

Xiong [8] investigated Al-Si-Fe-Ba alloy production using coal fly ash by electro-thermal method. Ma [9] made Al-Si-Fe alloy from the mixture of coal fly ash, bauxite, hematite, silica, and fluorite, but the generated Al-Si-Fe alloy contains a lot of carbides. During the reduction process of coal fly ash, iron promotes the formation of Al-Si-Fe phase and the decomposition of carbides [10]. Silicon in the system improves the thermodynamic reduction conditions of alumina [11] and reduces the vaporization of aluminum [12, 13]. Rapid heating and long reaction time at high temperature can increase metal recovery, and reduce the deposition of carbides at the bottom of furnace [14].

Silicothermic reduction of dolomite under vacuum suggests that the reaction is controlled by the solid-state diffusion of reactants with the Jander and Ginstling–Brounshtein model providing the best representation of the process kinetics [15]. Aluminothermic reduction of the mixture of calcined magnesite in vacuum showed that the overall reaction rate was controlled by interfacial chemical reaction in the early stage, following by the boundary diffusion of molten aluminum and gaseous magnesium in the final stage [16]. CaF_2 plays a catalytic

*Corresponding author: yqcy@163.com

https://doi.org/10.2298/JMMB210118038Y

role in the reduction of magnesia [17]. In-situ observation of the aluminothermic reduction of magnesia showed that the penetration of molten aluminum took place through cracks of the alumina film. The reduction proceeded after the penetration of molten aluminum into the magnesium oxide phase [18]. As a reductant, aluminum allows the reduction of MgO at lower temperatures than that of ferrosilicon [19].

Reduction rate of MgO using aluminum alloy as a reductant was higher than that of aluminum powder, and increased with the increasing aluminum content [20, 21]. Although research on the aluminothermic reduction of magnesia with aluminum alloy has been done, aluminum alloy was prepared by mixing aluminum and other metals. Few studies about magnesium production with Al-Si-Fe alloy directly from coal fly ash have been reported. Aluminum and silicon are both active ingredients in Al-Si-Fe alloy. It is necessary to recover aluminum and silicon from coal fly ash as much as possible. In this work, thermodynamic analysis was made to illustrate the feasibility of carbothermic reduction of Al_2O_3, SiO_2 and Fe_2O_3 of fly ash and thermal reduction of magnesia. Effect of temperature, time, and carbon dosage on the recovery rate of Al, Si, and Fe under atmospheric pressure was investigated and optimized. In addition, the effect of temperature on the thermal reduction of magnesia in vacuum is also discussed.

2. Experimental

2.1. Raw Materials

Fly ash from Shanxi province in China was ground and passed through 100-mesh sieve. SEM image (Fig. 1) reveals that coal fly ash is composed of many spherical and irregular particles. Chemical composition of coal fly ash was obtained by chemical analysis as shown in Tab. 1. Content of Al_2O_3, SiO_2, and Fe_2O_3 reached 20.73%, 54.47%, and 8.37%, respectively. XRD pattern (Fig. 2) indicates that the main crystallized mineral phases consist of quartz (SiO_2), mullite ($3Al_2O_3{\cdot}2SiO_2$), and hematite (Fe_2O_3). Analytic purity MgO from Tianjin Fengchuan chemical reagent Technology Co., Ltd and charcoal from Kunming Iron and Steel Holding Co., Ltd was used as a magnesium source and a reductant, respectively. Industrial parameters of charcoal, such as moisture (M_{ad}), volatiles (V_{ad}), coal ash (A_{ad}), fixed carbon (FC_{ad}), and ash composition, were shown in Tab. 2.

2.2. Experimental setup

Experiments were carried out in a high-frequency induction furnace and vacuum furnace, respectively, and the schematic diagram of the setup is shown in Fig. 3. The high-frequency induction furnace includes power supply unit, infrared radiation apparatus, and heating device. The power supply unit provides both power and electrical control. Infrared radiation apparatus is used for the temperature measurement. The heating device consists of graphite crucible, refractory filler, insulation layer, and heating coil. The heating coil is cooled by circulating water. As shown in Fig. 3 (b), the reactor was provided with a central removable tube that permitted inserting a thermocouple in order to know the

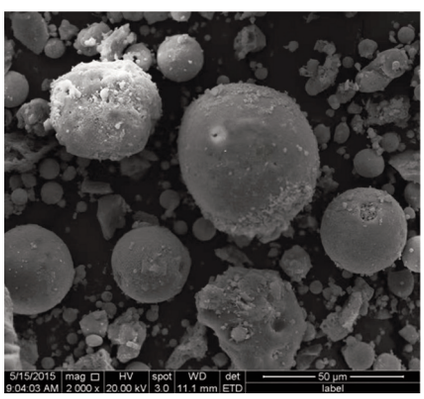

Figure 1. *SEM image of coal fly ash*

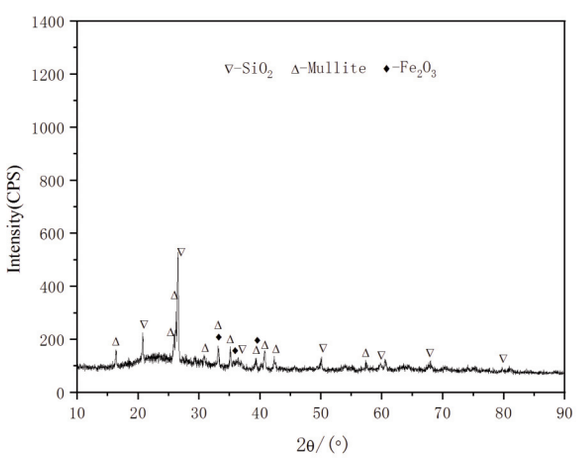

Figure 2. *XRD pattern of coal fly ash*

Table 1. *Chemical composition of coal fly ash*

Composition	Al_2O_3	SiO_2	Fe_2O_3	CaO	TiO_2	MgO	S	C
Content (wt.%)	20.73	54.47	8.34	3.83	2.51	1.12	0.08	1.63

Table 2. *Industrial analysis of charcoal (air-dry basis)*

Property index	M_{ad}	A_{ad}	V_{ad}	FC_{ad}	Ash composition					
					Fe_2O_3	Al_2O_3	CaO	TiO_2	MgO	SiO_2
Index value (wt. %)	13.0	5.61	6.55	87.84	1.32	0.12	24.32	0.05	4.03	3.67

temperature in the reaction zone by means of a digital thermometer. The zone for the collection of the reaction products consisted of a boxlike collecting plate where the reaction products were condensed and a washing trapper for the collection of gas products.

2.3. Experimental procedures

Preparation of Al-Si-Fe alloy was carried out in a high-frequency induction furnace with the maximum temperature of 2473K. Previous works proved that the refractory filler would melt if the heating time was more than half an hour at 2473K. Therefore, the reaction temperature should be kept below 2473K. Raw materials have to be pelletized to achieve good gas permeability. 30.16g of charcoal and 6.51g of binder (calcium lignosulphonate) on the basis of 100g of coal fly ash were well mixed, and well proportionated ingredients were combined till the required consistency was achieved. The mixture was compressed into the cylindrical pellets (Φ10×15mm) under pressure of 30MPa, and dried at 150°C for 24h to remove moisture. A graphite crucible loaded with pellets was placed into the furnace. Carbothermic reduction of fly ash proceeded continuously for 40min to ensure a complete reduction of fly ash. After the experiment, the graphite crucible was immediately removed from the furnace and cooled at room temperature. There is a slag layer on the surface of the alloy. Effect of air on the alloy can be neglected during the rapid cooling. The graphite crucible was cut open to collect Al-Si-Fe alloy.

Preparation of magnesium was carried out in the vacuum furnace. The obtained Al-Si-Fe alloy was broken, ground, and passed through 100-mesh sieve. The alloy particles were mixed with magnesia evenly with mass ratio of 1:2.2 and total mass of 50.8g. Cylindrical pellets were made in a similar way as fly ash pellets do. A corundum crucible loaded with cylindrical pellets was put into the heating area of the vacuum furnace. Then, a condensing device was placed above the heating area. Turn on the cooling water and air pump. After 10 minutes the vacuum furnace started for heating. Reduction of magnesia was carried out under conditions that reaction time is 2h, vacuum degree is 5-15Pa, and temperature is 1373k, 1423k, and 1473k, respectively. Magnesium was taken out after natural cooling in the vacuum furnace.

2.4. Analysis methods

Scanning Electron Microscopy with an energy dispersive spectrometer (SEM-EDS: JEOL, JSM-6510LV) was used to examine the morphology and the surface element content of Al-Si-Fe alloy and magnesium. Slag after thermal reduction of magnesia was examined by X-ray diffractometer (XRD: PANALYTICAL, EMPYREAN, Cu-Kα radiation). Composition of Al-Si-Fe alloy was determined by chemical analysis. Carbon dosage is expressed by carbon ratio of the practical and theoretical carbon dosage, respectively. The theoretical carbon dosage was the stoichiometric amount of carbon for the reduction of alumina, silica, and iron oxide in coal fly ash. Recovery rates of aluminum, silicon, and iron are calculated as follows:

$$X_{Al,Si,Fe} = \frac{M}{M_0} \cdot 100\% \quad (1)$$

Where M is the content of Al, Si, and Fe in Al-Si-Fe alloy, respectively; M_0 is the content of Al, Si, Fe in coal fly ash, respectively. According to the results, only a small amount of SiC is produced. In order to determine the recovery rate of SiC, combustion of Al-Si-Fe alloy particles was conducted, then following the determination of carbon content with carbon sulphur analyser (LECO, Cs230, USA). Accordingly, the content of SiC is obtained. The recovery rate of SiC can be quantitatively derived by:

$$X_{SiC} = \frac{M_{alloy} \cdot W_{SiC} \cdot \frac{28}{40}}{M_{fly\ ash} \cdot W_{SiO_2} \cdot \frac{28}{60}} \quad (2)$$

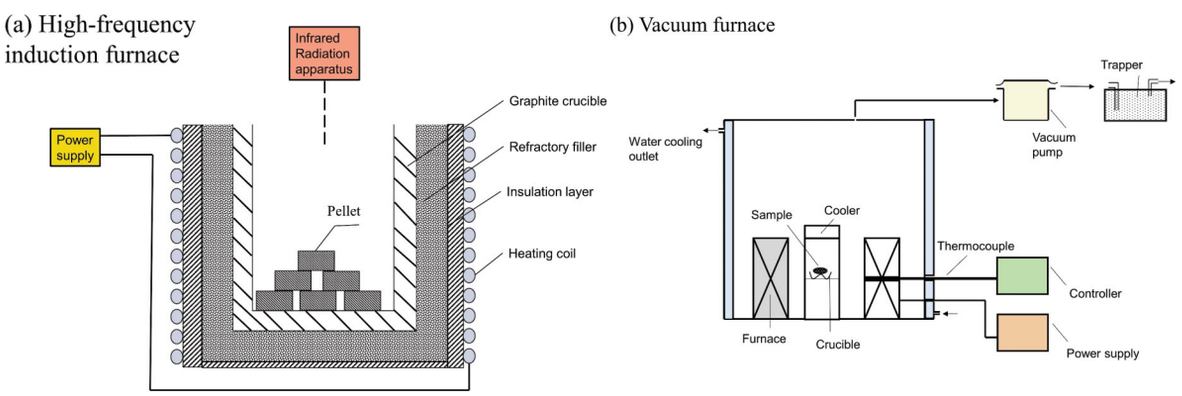

Figure 3. *Schematic diagram of experimental setups: (a) High-frequency induction furnace; (b) Vacuum furnace*

Where M_{alloy} is the mass of Al-Si-Fe alloy, $M_{fly\ ash}$ is the mass of fly ash, and W_{SiC} and W_{SiO2} are the contents of SiC in Al-Si-Fe alloy and SiO_2 in fly ash, respectively.

3. Thermodynamic analysis

Carbothermic reduction of coal fly ash is a complex heterogeneous process that takes place over a series of individual reactions concerning metals to be extracted. Coal fly ash contains massive alumina and silica, and little iron oxide as shown in Tab. 2. It is necessary to make a thermodynamic assessment of possible reactions of Al_2O_3, SiO_2 and Fe_2O_3 in the reduction of coal fly ash under atmospheric pressure and the reduction of MgO using the generated Al-Si-Fe alloy in vacuum.

Fitting formulas obtained on the basis of thermodynamic calculation for the Gibbs free energy versus temperature of the reactions are shown in Tab. 3, and diagrams of the Gibbs free energy change for these reactions as function of temperature are presented in Fig. 4. It is found in Fig. 4(a) that most of reactions show negative correlations with the increase of temperature except the reaction (10). More and more AlN can be produced after 1969.14K by the reaction (1). The generated AlN will react with SiC by the reaction (2). Feasibility of AlN produced by the reaction (10) weakens with the increase of temperature. Al_4C_3 and Al_4CO_4 are intermediate products during the reduction of Al_2O_3. Initial temperatures of the reactions (2) and (5) are 1346.47K and 2480.45K, respectively. It can be found that the generated AlN can lower down the reduction temperature of SiC by 1134K. Much the same is happening for the reactions (6) and (7).

Table 3. *Possible reactions and the fitting formula of the Gibbs free energy versus temperature*

Number	Reaction equations	Fitting formula of Gibbs free energy/kJ•mol^{-1}
-1	$Al_2O_3+3C+N_2(g)=2AlN+3CO(g)$	Δ_rG^θ = 678.3700-0.3445T
-2	$2AlN+2SiC+O_2(g)=2Al+2Si+N_2(g)+2CO(g)$	Δ_rG^θ=606.0479-0.4501T
-3	$2Al_2O_3+3C=Al_4CO_4+2CO(g)$	Δ_rG^θ= 794.3520-0.3665T
-4	$Al_4CO_4+6C=Al_4C_3+4CO(g)$	Δ_rG^θ=1612.7542-0.6954T
-5	$Al_2O_3+3SiC=2Al+3Si+3CO(g)$	Δ_rG^θ= 1605.8461-0.6474T
-6	$3SiO_2+2Al_4C_3=8Al+3Si+6CO(g)$	Δ_rG^θ=2578.9569-1.2481T
-7	$Al_2O_3+Al_4C_3=6Al+3CO(g)$	Δ_rG^θ= 1599.5511-0.6743T
-8	$Al_2O_3+3Si=2Al+3SiO(g)$	Δ_rG^θ= 1302.9962-0.5134T
-9	$Al_2O_3+2C=Al_2O(g)+2CO(g)$	Δ_rG^θ= 1263.5383-0.5370T
-10	$Al_2O(g)+CO(g)+N_2(g)=2AlN+CO_2(g)$	Δ_rG^θ =-749.6009+ 0.3622T
-11	$SiO_2+2C=Si+2CO(g)$	Δ_rG^θ= 683.6556-0.3523T
-12	$SiO_2+3C=SiC+2CO(g)$	Δ_rG^θ= 593.5582-0.3293T
-13	$SiO_2+SiC=3Si+2CO(g)$	Δ_rG^θ= 863.8488-0.3981T
-14	$SiO_2+C=SiO(g)+CO(g)$	Δ_rG^θ = 672.8021-0.3305T
-15	$SiC+O_2(g)=SiO(g)+CO(g)$	Δ_rG^θ = -152.0898 -0.1712T
-16	$SiO_2+SiC=2SiO(g)+C$	Δ_rG^θ = 752.0456-0.3316T
-17	$SiO(g)+2C=SiC+CO(g)$	Δ_rG^θ = -79.2431+ 0.0011T
-18	$Fe_2O_3+3C=2Fe+3CO(g)$	Δ_rG^θ = 464.3454- 0.5063T
-19	$SiO_2+2C+3Fe=Fe_3Si+2CO(g)$	Δ_rG^θ =534.4661- 0.3123T (873.15K<T<2073.15K)
		Δ_rG^θ = -626.5703+ 0.2558T (2073.15K <T<2473.15K)
-20	$SiO_2+2C+Fe=FeSi+2CO(g)$	Δ_rG^θ = 603.7589-0.3471T
-21	$Fe_3Si+2Si=3FeSi$	Δ_rG^θ=-162.1765+ 0.0353T(873.15K<T<1673.15K)
		Δ_rG^θ =797.8248-0.4780T(1873.15K <T<2473.15K)
-22	$2Al + 3MgO = Al_2O_3 + 3Mg_{(g)}$	Δ_rG^θ =519.7749-0.2961T (P=1×10^{5}Pa)
		Δ_rG^θ =519.7749-0.4684T (P=1×10^{2}Pa)
		Δ_rG^θ =519.7749-0.5259T (P=1×10^{1}Pa)
-23	$Si + 2MgO = SiO_2 + 2Mg_{(g)}$	Δ_rG^θ =553.2340-0.2309T (P=1×10^{5}Pa)
		Δ_rG^θ =553.2340-0.3458T (P=1×10^{2}Pa)
		Δ_rG^θ =553.2340-0.3841T (P=1×10^{1}Pa)

Compared with Al_2O_3, SiO_2 can reduce the reduction temperature of Al_4C_3 by 309K. Production of gaseous SiO and Al_2O by reactions (8) and (9) proceeds more and more with the increase of temperature.

As shown in Fig. 4(b), the Gibbs free energy change of the reactions (11)-(16), (18) and (20) show negative correlation with the increase of temperature meaning the increase of reaction trend of these reactions. An approximately level line of the reaction (17) below baseline indicates that production of SiC can occur within the temperature range of 873K-2473K. Diagrams of the reactions (19) and (21) present a polygonal shape with opposite direction after 2073.15K and 1873.15K, respectively, which indicate a weakening trend of the reaction (19) and an increasing trend of the reaction (21) with the increase of temperature, respectively. It is found that the reduction temperature of silica decreases clearly with the presence of iron by comparing with the reactions (11) and (19).

Fig. 4(c) indicates that $\Delta_r G_m$ decreases with the increase of temperature and the decrease of vacuum degree, which contribute to the reactions (22) and (23). The initial temperature of the reaction (22) is 882.8K at 10Pa. In other words, MgO can be reduced into magnesium by aluminum above 882.8K. In comparison with the normal pressure, the initial temperature is reduced by 870.9K. Similarly, the initial temperature of the reaction (23) is 1440.34K at 10Pa and 2395.99K in the atmosphere, respectively. It is found that the thermodynamics conditions of magnesium production are improved greatly in vacuum. Aluminum lowers down the reduction temperature of magnesia greatly compared with silicon.

4. Results and discussion

4.1. Preparation of Al-Si-Fe alloy

4.1.1. Effect of temperature on recovery rate

Effects of temperature in the range of 2273K - 2423K on the recovery rate of aluminum, silicon and iron are shown in Fig. 5. Other conditions are that time is 20min, and the carbon ratio is 0.85. There is an obvious change of descend firstly then ascend for the recovery rate of iron with the increase of temperature, and the recovery rate is more than 100% because of the reduction of Fe_2O_3 in charcoal. Meanwhile, the generated iron may be lost in the molten slag due to the negative deviation of activity [22], leading to the change of recovery rate of iron. More and more silicon is produced with the increase of temperature by the reactions (6) and (13). Evaporation

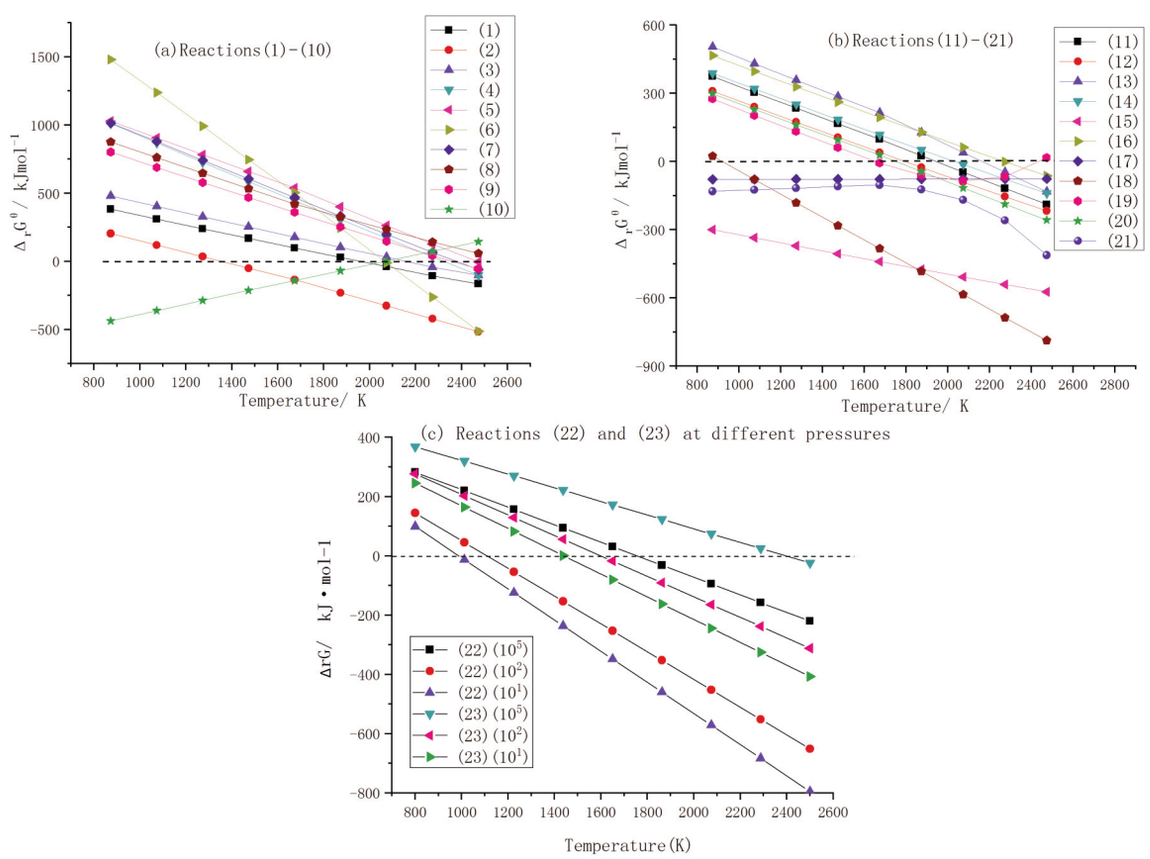

Figure 4. *Diagrams of the Gibbs free energy as functions of temperature: (a) Reactions (1)-(10); (b) Reactions (11)-(21); (c) Reactions (22) and (23) at different pressures*

loss of SiO by the reactions (14)-(16) accounts for small part of the total silicon. Recovery rate of aluminum increases significantly with the increase of temperature from 2273 to 2373 K, but an obvious decrease appeared above 2373 K with a recovery rate of 53.29%. This is largely due to the evaporation of gaseous Al_2O caused by the reaction (9). All those factors point to 2373K as the suitable temperature.

4.1.2. Effect of time on recovery rate

Fig. 6 shows the curves for the recovery rate of aluminum, silicon, and iron versus time under conditions of temperature 2323K and carbon ratio 0.85. The recovery rate of iron is more than 100% because small amount of iron in charcoal is reduced. The recovery rate of iron shows a trend of rising, dropping, and rising again with the increase of time, meaning unstable dissolution of iron in slag caused by foaming. The recovery rates of aluminum and silicon both increase with the increase of time and decrease as time is more than 30min, and the maximums are 63.75% and 75.82%, respectively. The reduced sample is liquid at high temperature. If gaseous Al_2O and SiO volatilize from the liquid phase, bubbles with the desired size are required. From a kinetic point of view, it will take some time for the transportation of gaseous Al_2O and SiO in liquid phase and the growth of bubbles. Extending time will promote the volatilization of gaseous Al_2O and SiO, inevitably causing the decrease of recovery rate of aluminum and silicon. The optimal reaction time is 20min.

4.1.3. Effect of carbon dosage on recovery rate

Previous research [23] showed that excess carbon easily leaded to the formation of oxycarbide and carbide. So, the effects of carbon ratio in the range of 0.80 - 0.95 on the recovery rate of aluminum, silicon, and iron were investigated. Other conditions are that temperature is 2323K, and time is 20min. The results are shown in Fig. 7. There is a small amount of Fe_2O_3 in charcoal. Accordingly, the increase of carbon ratio means the increase of Fe_2O_3 addition. However, the recovery rate of iron doesn't show a continuous increase. It can be inferred that the iron loss by molten slag is far more than the iron oxide addition by charcoal. Recovery rate of silicon shows a slow increase up to the maximum of 76.5% at a carbon ratio of 0.95. A similar trend of variation in the recovery rate of iron and aluminum is observed. A more reasonable carbon ration is 0.90. Carbon dosage plays an important role on the formation of carbides, which inevitably influence the composition of the Al-Si-Fe alloy. As shown in Fig. 7, a slight increase for the recovery rate of SiC appears with the increasing carbon ratio. About 5% of SiO_2 in fly ash is transformed into SiC.

4.1.4. Phase composition and surface morphology analysis

As shown in Fig. 8, the Al-Si-Fe alloy contains Al_9FeSi_3, Si, Al, and SiC. No Al_4C_3 was found.

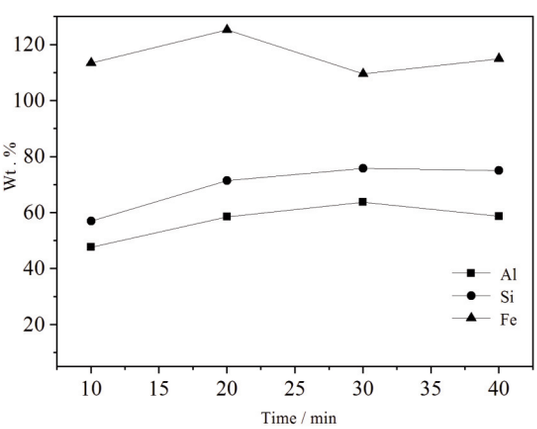

Figure 6. *Effect of time on the recovery rate of aluminum, silicon, and iron*

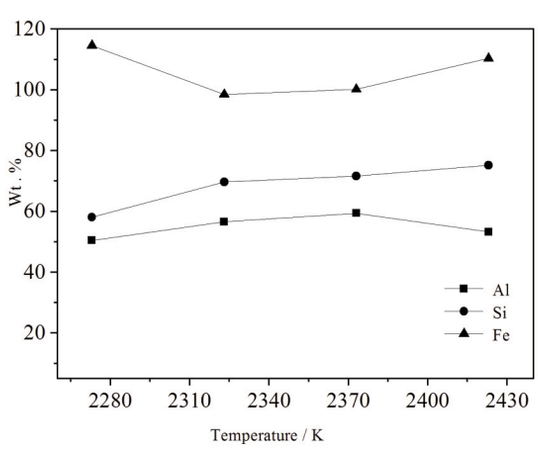

Figure 5. *Effect of temperature on the recovery rate of aluminum, silicon, and iron*

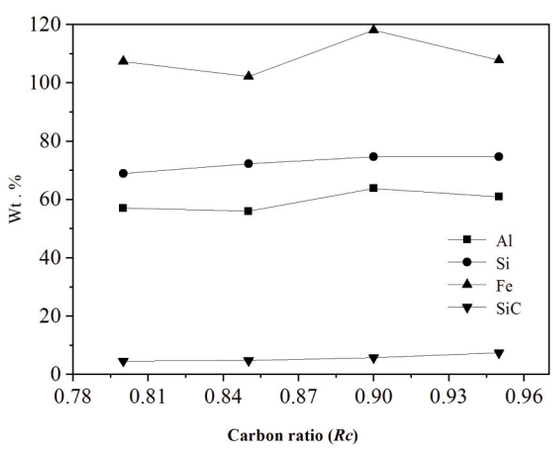

Figure 7. *Effect of carbon ratio on the recovery rate of aluminum, silicon, iron, and silicon carbide*

Although there is no reducibility for SiC, SiC is a small proportion because the recovery rate of SiC is about 5% as shown in Fig. 7. Fig. 9(a) presents the cross-section morphology of Al-Si-Fe alloy after carbothermic reduction of coal fly ash under the optimal conditions. The alloy profile shows dark grey, light grey, and silvery white, which are labeled as areas (1), (2), and (3), respectively. EDS of three areas are shown in Fig. 9 (b), and the elemental compositions are shown in Tab. 4. It can be found that elements Al, Si, and C are in the area (1). The calculated Si/C atomic ratio is 1.3, which is more than the theoretical value of SiC with Si/C atomic ratio of 1. It is inferred that there exists Al-Si alloy phase besides SiC. The predominant phase in the area (2) was Al-Si-Fe, while a small amount of Ca and Ti were also observed. Area (3) shows the Al-Si-Fe-Ti phase. Average content of the Al-Si-Fe alloy is shown in Tab. 5. It is found that Al, Si, and Fe are major components in the product of carbothermic reduction of coal fly ash as well as to its raw ingredients, but Ca, Ti, and C represent a tiny fraction.

4.2. Preparation of magnesium

4.2.1. Phases analysis of slag

Thermal reduction of magnesia was carried out using the generated Al-Si-Fe alloy to prepare Mg in the temperature range of 1373K-1473K at 10Pa. Active components of aluminum and silicon both play a role in the reduction of magnesia. The generated slag was characterized by XRD (Fig. 10). At 1373k, it is observed that the phases are $MgAl_2O_3$, Mg_2SiO_4, MgO, Si, and $FeSi_2$. Diffraction peak of aluminum disappeared, meaning that the aluminothermic reduction of magnesia by reaction (22) took place. The generated Al_2O_3 reacts with unreacted MgO to produce $MgAl_2O_3$. Diffraction peak intensity of silicon and magnesia decreases with the increase of temperature. It is deduced that more and more silicon reacts with MgO. The result is consistent with the Gibbs free energy change of the reaction (23). Accordingly, the generated SiO_2 reacts with the unreacted MgO to produce Mg_2SiO_4. At 10Pa the initial temperatures of the reactions (22) and (23) are 988.35K and 1440.34K, respectively. Aluminum lowers down the reduction temperature of magnesia significantly compared with silicon.

As shown in Fig. 10, enhanced diffraction peak intensity of Mg_2SiO_4 and weakened diffraction peak intensity of MgO, Si, and $MgAl_2O_4$ were observed with the increase of temperature, meaning that high temperature favors the occurrence of the reaction (23). No aluminum but silicon was left in the slag, which was coincident with silicothermic reduction of magnesia using ferrosilicon [24]. Activity of aluminum is obviously more than that of silicon, and aluminum reacts with magnesia completely. If aluminum powder is used as reductant alone, alumina film impedes the aluminothermic reduction of magnesia [25]. The aluminothermic reduction of magnesia took place only after the stress formed during phase transformation could break up the alumina film at the elevated temperature. As shown in Fig. 9, alumina film was not found. Obviously, the aluminothermic reduction of magnesia with Al-Si-Fe alloy is better than aluminum powder.

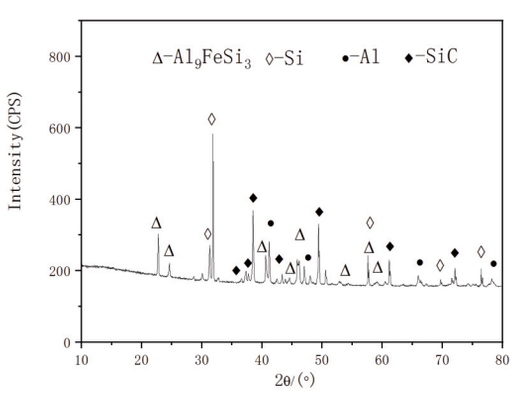

Figure 8. *XRD pattern of Al-Si-Fe alloy*

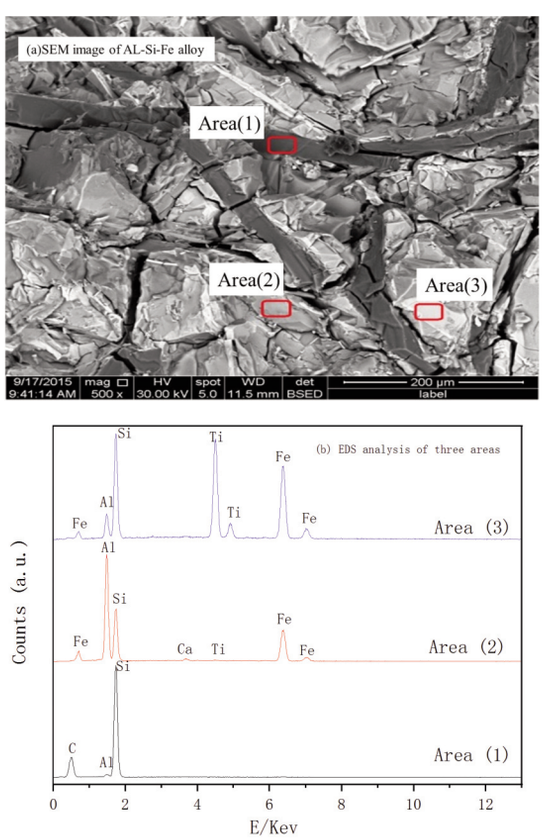

Figure 9. *SEM-EDS analysis of Al-Si-Fe alloy: (a)SEM image of Al-Si-Fe alloy; (b) EDS analysis of three areas*

4.2.2. Surface morphology of magnesium

The elemental compositions are shown in Tab. 4.

Surface morphology of magnesium produced at 1423K was characterized by SEM as shown in Fig. 11. Magnesium grains exhibit columnar growth. Internal porous structure enlarges the surface roughness. EDS analysis of the micro-area shows that the elemental compositions include magnesium and oxygen. Chemical analysis results show that the content of magnesium is 98.46% (Tab. 6). Small amount of oxygen was caused by the oxidation on the surface of magnesium. Rapid condensation caused partial supersaturation of magnesium vapor, and magnesium nuclei formed and deposited. According to the classical nucleation theory [26, 27], the nucleation rate is more than the growth rate at a high undercooling degree. Alternatively, the nucleation rate is less than the growth rate at a low undercooling degree. Under the circumstances the magnesium nuclei grow along the direction of crystal edge or vertex, and tiny grains are also adsorbed. Consequently, columnar crystal of magnesium formed with large grain size and flat surface.

4.3. Comparative analysis of aluminothermic reduction process and Pidgeon process

In aluminothermic reduction process, aluminum alloy has an advantage over aluminum powder because aluminum powder is easily oxidized. Additionally, when silicon is substituted with iron, activity of aluminum in Al-Si-Fe alloy increases [22]. Pidgeon process is a typical magnesium production with the reductant of 75% ferrosilicon. The utilization rate of reductant, energy and raw materials consumption are the crucial criteria with which to judge the reduction performance. A comparison of aluminothermic reduction process with Al-Si-Fe alloy and Pidgeon process with 75% ferrosilicon was made and analyzed.

On average, the temperature of the aluminothermic reduction of magnesia is thus expected to be lower than that of the Pidgeon process, which is beneficial in terms of extending the service life of the reduction pot and saving energy [28]. If aluminum addition exceeds the stoichiometric amount by the reaction (22), MgO in the form of $MgO{\cdot}Al_2O_3$ that formed in an earlier stage will be partially reduced to magnesium, but the reaction temperature will be higher [29]. For $2MgO{\cdot}SiO_2$, they are also the same situation. On the other hand, products of forsterite (Mg_2SiO_4) and spinel ($MgAl_2O_4$) are refractories which can be reused elsewhere. CaO is a slag-forming compound in Pidgeon process. When CaO is added in aluminothermic reduction of magnesia, the reaction of reduction process was $CaO+6MgO+4Al=CaO{\cdot}2Al_2O_3+6Mg$. Obviously CaO plays the part similar to that in the Pidgeon process. The reduction residue that the main phase of $CaO{\cdot}2Al_2O_3$ leached in alkaline solution can be used for producing sodium aluminate-the raw material for special alumina [30].

In Fig. 8 diffraction peak of aluminum disappears, suggesting that aluminum in Al-Si-Fe alloy participates in the reduction of magnesia completely. Content of aluminum 33.12% (Tab. 5) represents 25.76% Si based on the same amount of magnesium according to the reactions (22) and (23). Together with the original 48.73% silicon (Tab. 5), the total silicon content 74.49% is close to the 75% ferrosilicon. Moreover, the direct carbothermic reduction of alumina can substantially improve the sustainability of primary aluminum production, leading to energy savings of up to 21%, greenhouse gas emissions reductions of up to 52%, and plant

Table 5. *Chemical composition of Al-Si-Fe alloy*

Composition	Al	Si	Fe	Ti	Ca	C
Wt.%	33.12	48.73	6.41	1.56	2.03	1.71

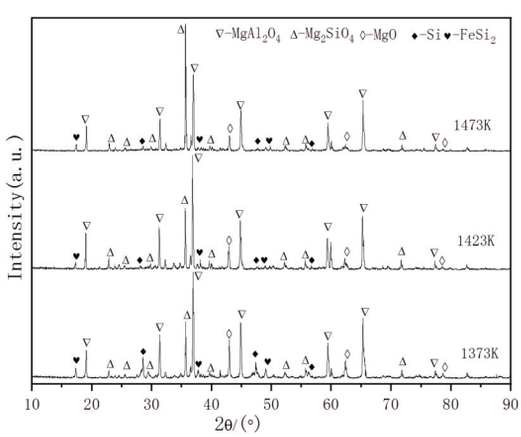

Figure 10. *Diffraction pattern of reducing slag at different temperatures*

Table 4. *Elemental composition of three areas*

Area (1)			Area (2)			Area (3)		
Element	wt.%	at.%	Element	wt.%	at.%	Element	wt.%	at.%
Al	1.94	1.49	Al	40.77	47.93	Al	7.77	11.39
Si	72.06	53.48	Si	32.38	36.57	Si	28.56	40.25
C	26.00	45.03	Fe	25.50	14.48	Fe	36.20	25.66
			Ti	0.40	0.26	Ti	27.47	22.70
			Ca	0.95	0.75			

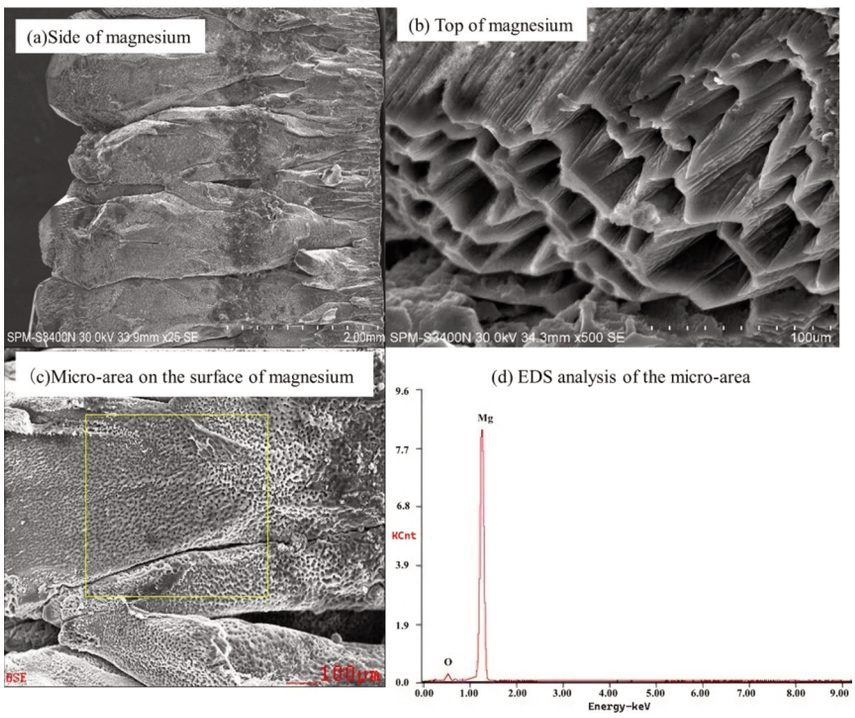

Figure 11. *SEM-EDS analysis of magnesium*

Table 6. *Chemical composition of magnesium*

Composition	Mg	O	Others
wt.%	98.46	1.39	0.15

capital costs reductions of up to 50% [31].

Ferrosilicon, mainly produced in a ferroalloy plant in China, is an important material for magnesium production. In China, ferrosilicon is produced using iron oxide and quartz as raw materials and coke as reductant [32]. Considerable quartz mineral resource is consumed. Meanwhile, most ash disposal methods ultimately lead to the dumping of coal fly ash on open land. Statistically every tons of coal fly ash occupy 0.27 - 0.33 hectares of land [33]. If inhaled, coal fly ash particles with a diameter less than 7μm can penetrate upper respiratory tract, and cause cancer and nervous system impacts [34]. Coal fly ash can even reach the sub-soil and ultimately cause siltation, clog natural drainage systems and contaminate the ground water with heavy metals. Recycling coal fly ash to produce Al-Si-Fe alloy is a good alternative to disposal, which can achieve significant economic and environmental benefits as well. Therefore, Al-Si-Fe alloy is a potential replacement of 75% ferrosilicon as reductant in magnesium production.

5. Conclusions

(1) Thermodynamic analysis was conducted based on the carbothermic reduction of coal fly ash under normal pressure and thermal reduction of magnesia in vacuum. AlN and SiO_2 can lower down the reduction temperature of SiC and Al_4C_3, respectively. Increase of temperature and decrease of vacuum degree promotes the thermal reduction of magnesia.

(2) The optimal recovery rate of aluminum, silicon and iron was obtained under conditions of temperature 2373K, reaction 20min, and carbon ratio 0.9. Al-Si-Fe alloy contains 33.12% Al, 48.73% Si, and 6.41% Fe. The phase compositions include Al_9FeSi_3, Si, Al, and SiC. No Al_4C_3 is found.

(3) Magnesium with content of 98.46% was prepared using Al-Si-Fe alloy from carbothermic reduction of coal fly ash as reductant. The nucleation rate is less than the growth rate at a low undercooling degree when magnesium vapor is condensed. Al-Si-Fe alloy is a potential replacement of 75% ferrosilicon in magnesium production.

Acknowledgements

This work was financially supported by the National Natural Science Foundation of China (No. 51864025).

References

[1] W.D. Xie, J. Chen, H. Wang, X. Zhang, X.D. Peng, Y. Yang, Rare Met., 35(2)(2016) 192-197.

[2] J.H. Guo, D.X. Fu, J.B. Han, Z.H. Ji, Z.H. Dou, T.A. Zhang, J. Min. Metall. B., 56(3)(2020)379-386,

[3] R.L. Thayer, R. Neelameggham, JOM, 53(8)(2001) 15-

17.
[4] F. Cherubini, M. Raugei, S. Ulgiati, Resour. Conserv. Recy., 52(8-9)(2008) 1093-1100.
[5] J.D. Du, W.J. Han, Y.H. Peng, J. Clean. Prod., 18(2)(2010) 112-119.
[6] H.Z. Ma, Z.X. Wang, Y.N. Wang, D.D. Wang, Green Process. Synth., 9(2020) 164-170.
[7] J.B. Zhu, H. Yan, Int. J. Min. Metall. Mater., 24(3)(2017) 309-315.
[8] W.Q. Xiong, M. Xiong, J. Solid Waste. Tech. Manage., 36(1)(2010) 20-25.
[9] G.J. Ma, Y.B. Jin, D.B. Yang, Adv. Mater. Res., 291-294(2011) 1808-1811.
[10] X.T. Fu, X.J. Li, X. Zhang, Y. Zhao, J. Liu, World Nonferrous. Met., 1(2013) 40-42. (In Chinese)
[11] F. Zhang, M.J. Li, Ferro-alloys, 4(2003) 17-21. (in Chinese)
[12] J.A. Taylor, Procedia Mater. Sci., 1(2012) 19-33.
[13] C. Kemper, E. Balomenos, D. Panias, I. Paspaliaris, B. Friedrich, TMS2014 143rd Annual Meeting & Exhibition, February 16-20, San Diego, USA, 2014, p. 789-794.
[14] D. Yang, N.X. Feng, Y.W. Wang, X.L. Wu, Trans. Nonferrous Met. Soc. China., 20(1)(2010) 147-152.
[15] W. Wulandari, G.A. Brooks, M.A. Rhamdhani, B.J. Monaghan, Can. Metall. Quart., 53(1)(2014)17-25.
[16] D.X. Fu, Y.W. Wang, J.P. Peng, Y.Z. Di, S.H. Tao, N.X. Feng, Trans. Nonferrous Met. Soc. China., 24(8)(2014) 2677-2686.
[17] Y.W. Wang, J. You, N.X. Feng, W.X. Hu, Chin. J. Vacuum Sci. Tech., 32(2012) 889-895.
[18] J. Yang, M. Kuwabara, Z.Z. Liu, T. Asano, M. Sano, J. Iron Steel Inst. Jpn., 92(4)(2006) 239-245.
[19] M. Bugdayci, A. Turan, M. Alkan, O. Yucel, High Temp. Mater. Proc., 37(1)(2018) 1–8.
[20] J. You, Y.W. Wang, X.Z. Deng, K.J. Liu, Magnesium extraction from calcined dolomite by vacuum thermal reduction with solid waste of Al-Fe alloy, Chin. J. Vacuum Sci. tech., 36(4)(2016) 436-441(In Chinese).
[21] D.F. Fu, N.X. Feng, Y.W. Wang, J.P. Peng, Y.Z. Di, Trans. Nonferrous Met. Soc. China., 24 (3)(2014) 839-847.
[22] X.X. Wu, Nonferrous Metals, 52(2000) 72-74. (In Chinese)
[23] Q.C. Yu, H.B. Yuan, F.L. Zhu, H. Zhang, C. Wang, D.C. Liu, B. Yang, J. Cent. South Univ., 19(7)(2012) 1813−1816.
[24] R.Y. Xu, Production Technology of Magnesium Production by Silicothermic Method, Central South University Press, Chang Sha, 2002, p 102 (In Chinese).
[25] J. Yang, M. Kuwabara, Z.Z. Liu, T. Asano, M. Sano. ISIJ International., 46(2)(2006) 202-209.
[26] C. Ratsch, J.A. Venables, J. Vacuum Sci. Tech A: Vacuum, Surfaces, and Films, 21(5)(2003)S96-S109.
[27] M.S. Cao, Science and Technology of Ultrafine Particle Preparation, Harbin Institute of Technology Press, Harbin, 1995, p. 77 (In Chinese).
[28] Y.W. Wang, J. You, J.P. Peng, Y.Z. Di, JOM., 68(6)(2016) 1728-1736.
[29] Y.W. Wang, J.P. Peng, Y.Z. Di, N.X. Feng, M. Li. Chin. J. Vac. Sci. Technol., 33(7)(2013) 704-708. (in Chinese)
[30] W. Hu, N. Feng, Y. Wang, Z. Wang. Essential Readings in Magnesium Technology. Springer, Cham. 2016, p. 121
[31] E. Balomenos, D.I. Gerogiorgis, Encyclopedia of Aluminum and Its Alloys, Taylor & Francis Group, Abingdon, 2018, p. 207.
[32] A.S. Hauksdóttir, A. Gestsson, A. Vésteinsson, Control Eng. Pract., 10(4)(2002) 457–463.
[33] Z.T. Yao, X.S. Ji, P.K. Sarker, J.H. Tang, L.Q. Ge, M.S. Xia, Y.Q. Xi, Earth-Sci. Rev., 141(2015) 105–121.
[34] M.R. Senapati, Curr. Sci., 100(25)(2011) 1791-1794.

TERMIČKI PROCES PROIZVODNJE MAGNEZIJUMA SA Al-Si-Fe LEGUROM DOBIJENOM IZ UGLJENOG PEPELA: TERMODINAMIKA I EKSPERIMENTALNA ISPITIVANJA

Q.-C. Yu*, Y. Deng, S.-B. Yin, Z.-Y. Li

Glavna državna laboratorija za čisto iskorišćavanje resursa kompleksnih obojenih metala, Fakultet inženjerstva metalurgije i energije, Univerzitet za nauku i tehnologiju u Kunmingu, Kunming, NR Kina

Apstrakt

Odlaganje i skladištenje pepela prouzrokuje zagađenje okoline i ogroman gubitak vrednih metala. U ovom radu su ispitivane karbotermička redukcija pepela pod normalnim pritiskom da bi se proizvela Al-Si-Fe legura, kao i termička redukcija magnezijum oksida da bi se proizveo magnezijum u vakuumu sa Al-Si-Fe legurom. Uz to, površinska morfologija i sastav Al-Si-Fe legure i magnezijuma ispitivani su SEM-EDS i XRD metodom. Na osnovu termodinamičkih analiza ustanovljeno je da AlN i SiO_2 spuštaju temperature redukcije SiC i Al_4C_3, pojedinačno. Povećanje temperature i smanjenje stepena vakuuma potpomaže termičku redukciju magnezijum oksida. Rezultati su pokazali da je stopa iskorišćenja u opadajućem redosledu rangirala Fe, Si i Al. Gubitak gasovitih SiO i Al_2O isparavanjem smanjio je iskorišćenje Si i Al. Al-Si-Fe legura sa sadržajem 33.12% Al, 48.73% Si i 6.41% Fe dobijena je pod optimalnim uslovima. Magnezijum sa sadržajem od 94.87% pripremljen je uz korišćenje dobijene Al-Si-Fe legure kao reducenta. Brzina nukleacije je manja od brzine rasta tokom kondenzacije pare magnezijuma.

Ključne reči: *Ugljeni pepeo; Karbotermička redukcija; Aluminotermička redukcija; Al-Si-Fe legura; Magnezijum*